High-Resolution X-ray Imaging of a Globular Cluster Core: Compact Binaries in 47Tuc

Jonathan E. Grindlay,* Craig Heinke, Peter D. Edmonds, Stephen S. Murray

We have obtained high-resolution ($\lesssim$1″) deep x-ray images of the globular cluster 47Tucanae (NGC 104) with the Chandra X-ray Observatory to study the population of compact binaries in the high stellar density core. A 70-kilosecond exposure of the cluster reveals a centrally concentrated population of faint ($L_x \sim 10^{30-33}$ ergs per second) x-ray sources, with at least 108 located within the central 2′ × 2.5′ and $\gtrsim$ half with $L_x \lesssim 10^{30.5}$ ergs per second. All 15 millisecond pulsars (MSPs) recently located precisely by radio observations are identified, though 2 are unresolved by Chandra. The x-ray spectral and temporal characteristics, as well as initial optical identifications with the Hubble Space Telescope, suggest that $\gtrsim$50 percent are MSPs, about 30 percent are accreting white dwarfs, about 15 percent are main-sequence binaries in flare outbursts, and only two to three are quiescent low-mass x-ray binaries containing neutron stars, the conventional progenitors of MSPs. An upper limit of about 470 times the mass of the sun is derived for the mass of an accreting central black hole in the cluster. These observations provide the first x-ray "color-magnitude" diagram for a globular cluster and census of its compact object and binary population.

As the oldest stellar systems in the Milky Way Galaxy, globular clusters are laboratories for studies of stellar and dynamical evolution. The advantages of measurable ages and distances, both of which can be determined currently to ~10%, make globulars an especially attractive site for study of the evolution of stellar populations. The high stellar densities found in the cores of many globulars, with central values as high as $10^6 M_\odot$ pc^{-3} (*1*), implies that stellar interactions or near encounters can be relatively common—especially between stars and binary star systems. The role of binaries in cluster cores is dramatic: as a source of localized gravitational binding energy, they act as a dynamical heat source in the cluster core, stabilizing it against further collapse into a central black hole (*2*).

Compact binary stars, in which one member is either a white dwarf (WD) or a neutron star (NS), are markers of the extremes of stellar and binary evolution. Together with short-period binaries containing main-sequence stars, compact binaries interact with stars in globular cluster cores and affect the stellar populations directly. Stellar evolution within compact binaries containing either a WD or NS leads to mass transfer, and accretion onto the compact object makes them (and their progeny, MSPs) visible as persistent x-ray sources. X-ray flare emission and fainter continuous emission can also be detected from chromospherically active main-sequence (M-S) binaries, known as BY Draconis systems. Thus, x-ray observations are a particularly efficient way to study the compact binary population and the WD versus NS population in globulars.

A complete sample of luminous x-ray sources [L_x (2 to 10 keV) $\gtrsim 10^{36}$ erg s^{-1}] has been discovered in globular clusters in the Galaxy: one bright source is detected (though nearly 50% are transient) in each of 12 clusters, most with high central stellar density and metallicity (*3*). Type I x-ray bursts (*4*) have been detected from each, indicating all are NSs accreting from lower mass binary companions. This was also suggested by the ~3″-accuracy x-ray positions measured for six of them with the Einstein X-ray Observatory, which led to subsequent optical identifications for several and yielded radial offsets consistent with their being ~$2M_\odot$ objects (*5*). These 12 low-mass x-ray binaries (LMXBs) in the system of ~150 globulars in the Galaxy are, as originally suspected (*6*), ~200× more common (per unit mass) in globulars than in the Galaxy as a whole. Thus two-body stellar (tidal) interactions between a NS and M-S star, and the more probable exchange interactions of a NS with a pre-existing binary of two M-S stars, enhance LMXB production in globulars. The likely descendants of LMXBs, MSPs, in which the NS has been spun up to millisecond spin periods by accretion and becomes visible as a radio pulsar after the accretion phase ends (*7*), are also favored in globulars. Thus, the relative LMXB versus MSP populations in a globular can constrain the formation epoch of each and can influence whether alternative production channels are required for MSPs, such as accretion induced collapse (AIC) of massive WDs (to NSs), which could directly produce MSPs without a progenitor LMXB phase (*7*). In the relatively massive and high central density cluster 47Tuc (NGC 104), at least 20 MSPs are now detected, which implies a total population of ~100 to 200 in this cluster alone (*8*).

We obtained a 70-ks exposure of 47Tuc on universal time (U.T.) 16.31 to 17.22 March 2000 with the Chandra X-ray Observatory and the Advanced CCD Imaging Spectrometer-Imager (ACIS-I) at its focus (*9*). Our primary goal was to study the population of low-luminosity x-ray sources ($L_x \lesssim 10^{33-34}$ erg s^{-1}) discovered in this and other globulars (*10*) and originally suggested to be primarily accreting WDs and thus cataclysmic variables (CVs), together with a smaller population of the typically transient NS systems (LMXBs) in quiescence (quiescent LMXBs). Alternatively, the quiescent LMXB population may dominate the faint x-ray source population in globulars (*11*) and may be required to maintain the large MSP population if they are derived continuously from LMXBs (*7*). Thus, measurement and identification of a large sample of low-luminosity x-ray sources in 47Tuc, with its rich MSP population, can constrain the formation and evolution of MSPs as well as the relative populations of cluster WDs versus NSs, with implications for the cluster initial mass function. We present results from a 2.0′ × 2.5′ field centered on the cluster core that was chosen to include all of the 15 MSPs with precise positions (*12*). This analysis for an inscribed radius of 1′ = ~$2.6r_c$, where r_c is the cluster core radius (*13*), should include most compact binaries given their expected mass segregation (*2*). Results for the full 16′ × 16′ ACIS-I field will be presented in a subsequent paper.

Overview of source distributions. Previous x-ray studies of 47Tuc with the ROSAT (Rontgen Satellite) telescope and High-Resolution Imager (HRI) detector (*14*) revealed a population of nine sources with x-ray luminosity $L_x \sim 3$ to 100×10^{31} erg s^{-1}within ~1′ of the cluster center as well as underlying unresolved emission with total luminosity $L_x \sim 4 \times 10^{32}$ erg s^{-1}. The factor of $\gtrsim$10 improvements in angular and spectral resolution (to ~0.5″ and ~120 eV, respectively, with ACIS) achieved by Chandra over ROSAT enable detection of sources ~10 to 100× fainter. The spectral resolution enables comparison with x-ray spectra of known classes of source, whereas the exquisite po-

Harvard-Smithsonian Center for Astrophysics, 60 Garden Street, Cambridge, MA 02138, USA.

*To whom correspondence should be addressed. E-mail: josh@cfa.harvard.edu

sitional resolution permits much more detailed searches for optical counterparts with high-resolution Hubble Space Telescope (HST) images. Our deep exposure reached a sensitivity limit of $L_x \sim 6 \times 10^{29}$ erg s^{-1}for a threshold source with 3 counts (cts) (versus ~0.5 counts total background per source) detected at 90% confidence by the Chandra analysis tool Wavdetect (*15*) and assuming a soft thermal bremsstrahlung spectrum with temperature kT = 1 keV (most sources are "red," as discussed below) for comparison with the ROSAT results (*14*). The "true" color image of the cluster core as imaged by Chandra (Fig. 1) shows the range of source brightness and spectral color by combining counts detected in soft (0.5 to 1.2 keV; red), intermediate (1.2 to 2 keV; green), and hard (2 to 6 keV; blue) bands. Wavdetect finds 103 sources with total counts (in a 0.5- to 4.5-keV primary detection band) from 3 (detection threshold) to 5332 over the total 70 ks exposure. Five additional sources are found at the positions of MSPs Q, L, T, M, and C; Q, L, and T were missed by Wavdetect due to crowding, whereas M and C are only 3 and 1 count "detections," though precisely at the MSP positions, due to low exposure (~30%) on the detector gaps. Using the recently derived distance (5.0 kpc) and absorption for 47Tuc (*16*), we derive the luminosity distribution for the sources (Fig. 2). The complete list of 108 source positions and counts detected in several bands, as well as source identifications currently derived (some discussed below), are given in Web table 1 (available at *Science* Online at www.sciencemag.org/cgi/content/full/1061135/DC1).

The x-ray luminosity function increases at low values, with more than half the sources with $L_x \lesssim 3 \times 10^{30}$ erg s^{-1}. The 23 sources in the lowest L_x bin (2.5 to 7.5 cts; $L_x \sim 10^{30}$ erg s^{-1}) of the linear distribution form an incomplete set. From visual examination of the image as well as a ~500 count excess of total counts over Wavdetect source counts in the central core region (r $\lesssim 1r_c$), we estimate an additional $\gtrsim$100 sources with $L_x \lesssim 10^{30}$ erg s^{-1} are missed with Wavdetect due to crowding. Both a statistics-limited overlapping source detection algorithm (*17*) and a deeper ACIS-S exposure (with better low-energy sensitivity) are needed to constrain the number and types of these faintest core sources.

The sources appear to be of (at least) four types as marked with different symbols in Fig. 1. The distribution of source types can also be seen in the x-ray "color-magnitude" diagram (Fig. 3), which is possible to derive for the first time for a large population of x-ray sources in a single globular cluster.

Source identifications. Our analysis region of the cluster core was chosen to include the 15 MSPs with known positions (*12*) because 10 MSPs [including one in the globular cluster M28) have been detected in x-rays (*18*). Detection of even some in 47Tuc would enable a study of a population of cluster MSPs and their relation to both quiescent LMXBs and CVs. All 14 of the resolvable MSPs are detected [MSPs G and I, possibly a bound triple, have only 0.12″ separation (*12*)], with exposure-corrected counts ranging from 3 to 27 and thus $L_x \sim 10^{29.8-30.8}$ erg s^{-1}. Source identifications are possible because even the faintest (3 ct; $\gtrsim 2\sigma$ in Wavdetect) Chandra sources have positions with ~0.2″ uncertainties (1σ) due to the ~0.8″ Chandra image diameter (near the telescope axis) and 0.5″ ACIS pixel size. The precise (~0.001″) radio timing positions of the MSPs permit an astrometric solution for the Chandra source positions. Using seven of the brighter or best-resolved Chandra-MSP source candidates, the root mean square deviation between the Chandra and precise MSP positions is only 0.11″. Given a similarly precise Chandra-HST astrometric solution from our optically identified sources, precise optical searches for the MSP counterparts are now possible. Because the 14 resolved Chandra MSP candidates are all located near the center of the circles that mark the precise MSP positions (Fig. 1), the identifications are very likely. Although the probability that one of the estimated ~100 unresolved sources in the 23″ radius core is within 0.5″ of any MSP position is 0.05, this is applicable to only MSPs L and T (the only MSPs in the core not detected automatically with Wavdetect, and thus with positional uncertainties ~1 pixel = 0.5″ instead of Wavdetect centroid values of typically $\lesssim$0.1″ to 0.2″). The ACIS time resolution (nominal 3.2 s) does not permit analysis for pulsations, and the limited counts do not permit spectral analysis other than the determination of hardness ratios. The relatively narrow x-ray luminosity range implies a steep x-ray luminosity function, with typical L_x similar to the field MSPs detected outside of clusters (*18*), though the predominantly "red" x-ray colors (see below) are in contrast to some of the field MSPs with hard spectral components and the one in M28 with $L_x \sim 10^{32-33}$erg s^{-1}(*18*). Full details of the 47Tuc MSP x-ray source characteristics will be presented separately (*19*).

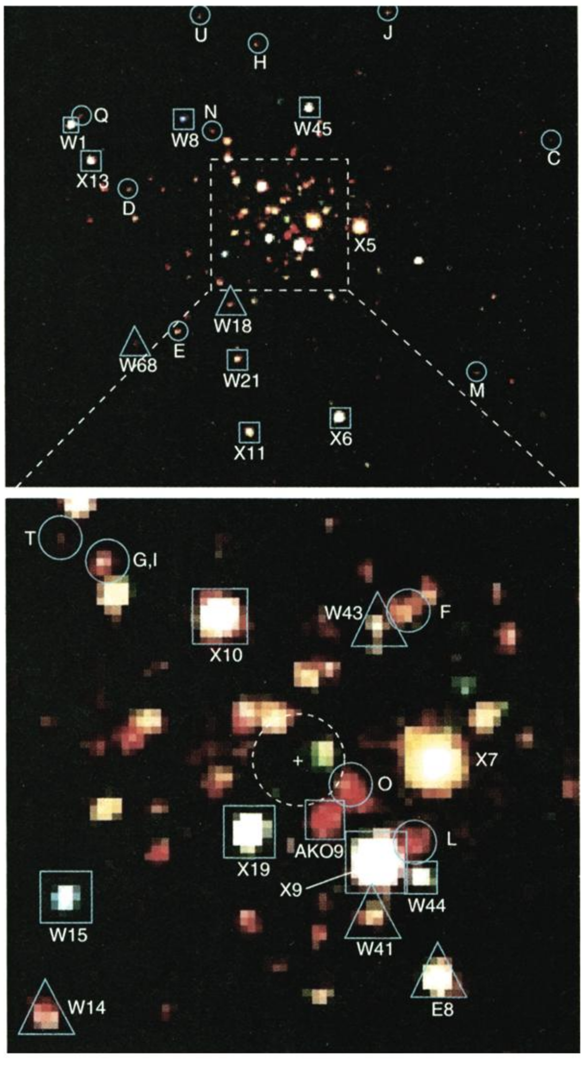

Fig. 1. X-ray color image of the central 2′ × 2.5′ of 47Tuc. Colors are derived from counts detected in soft (0.5 to 1.2 keV; red), intermediate (1.2 to 2 keV; green) and hard (2 to 6 keV; blue) bands with the I3 chip of the ACIS-I detector on Chandra. The pixel size (visible in enlargement of central core) is 0.4914″, and the enlarged central region is 35″ square. Source identifications are: MSPs (circles), marked with source letter names (*12*); quiescent LMXBs X5 and X7; CV candidates (squares), marked with ROSAT Xnumbers (*14*) or other Chandra Wnumbers; and possible flaring BY Dra systems, or M-S binaries (triangles), marked with E8 (*29*) or Chandra Wavdetect source numbers (Wnumbers). Precise positions, fluxes, hardness ratios, bright source spectra and variability are tabulated for all 108 sources shown here (73 unidentified are not labeled, for clarity) in our full-field analysis (*21*), with only key values given here in the text. The mean cluster center (*41*) and 3σ error (3″ radius dashed circle) are marked; other symbols (squares, etc.) are centered on sources but with sizes much greater than positional uncertainties.

Three other classes of sources are suggested by their x-ray spectra and temporal characteristics (Fig. 1). X5 and X7 are probable quiescent LMXBs, 13 sources are candidate CVs, and 6 sources appear to be M-S binaries detected in flare outbursts due to enhanced chromospheric activity. Each class is considered in turn to then enable constraints on the much larger unidentified population.

X5 and X7 are detected in the 0.5- to 4.5-keV medium-energy band with 4435 and 5332 counts (medcts) and have spectra dominated by soft black body components with kT = 0.31 and 0.29 keV, respectively. Their apparently constant black body luminosities [logL_x = 32.8; comparable to that detected with ROSAT (*14*)], implied emission radii of only ~0.8 km suggest they are quiescent LMXBs in which the x-ray emission is dominated by incandescence of the hot NS, slowly cooling from a previous accretion outburst phase. Using a hydrogen-atmosphere model, which modifies the opacity and temperature, as demonstrated with Chandra ACIS-S spectra for the field quiescent LMXB Cen X-4 (*20*), more realistic NS radii of ~10 km are derived (*21*). Our detailed spectral analysis of X5 and X7 also reveal a power law component (photon index 2.6 to 3) similar to that found for Cen X-4 and indicative of either residual accretion or a "propeller" spin-down luminosity source, as well as a possible line emission component [modeled (*21*) as a collisionally excited Raymond-Smith plasma with kT = 1 keV], indicative of a thin corona or perhaps wind from the system. The integrated fluxes for these two components are ~0.3 to 0.5 and ~0.2 of the black body component, respectively. Although a statistical test (Kolmogorov-Smirnov) on photon arrival times of X7 shows no significant variations in flux, X5 shows dramatic dips and possible eclipses, which may also be detected in the optical counterpart we have identified with HST (*22*). Both X5 and X7 are most probably quiescent LMXBs given their similar luminosities and spectra to those tabulated (*23*) for the six known NS-quiescent LMXB systems in the field. However, the hot gas and possible wind component may indicate that X5 and X7 are luminous, newly born MSPs ablating their companions and still optically thick to their radio emission because they are not among the currently located MSP sample (*12*). The lack of positive flux increases (i.e., flares versus the negative dips seen in X5) and otherwise constant flux would support but not require the MSP interpretation.

The 13 candidate CVs (Fig. 1) identified thus far in our HST identification program (*22*) have blue stellar counterparts indicative of accretion disks (though not all are yet determined to be variable). Apart from the quiescent LMXBs X5 and X7, all remaining ROSAT sources (X6, X9, X10, X11, X13, and X19) (*14*) within our analysis region (X4 is just outside) are CV candidates. Spectra have been fit (*21*) for the brightest eight sources (with medcts = 135 to 2402) and most are best fit with thermal bremsstrahlung with temperatures kT = 5 to 30 keV, typical of CVs (*24*). Soft black body components, as found for quiescent LMXBs, are generally not present. Three sources have unusually hard spectra: X6 is best fit with a thermal bremsstrahlung spectrum with kT ≳ 75 keV, and W8 and W15 both require similarly hard spectra but with internal self-absorption column densities of NH = 1.4 ± 0.4 and 0.7 ± 0.2 × 10^{22} cm^{-2}, respectively. Power law fits are equally acceptable for all three but with photon index α ~ 1.1 ± 0.1 (consistent with the slope of a thermal bremsstrahlung spectrum). Because such a flat power law index at low energies (<6 keV) is unprecedented for MSPs (for which the limited spectral data (*18*) indicate α ~ 2 to 3) or active galactic nuclei (AGN) with typical (*25*) α ~ 1.7, a thermal bremsstrahlung model is more likely. The excess NH in sources W8 and W15 is evident from their "blue" colors in Fig. 1 (absorption of soft counts), and might suggest they are background AGN, probably Seyfert 2 galaxies, even though the number

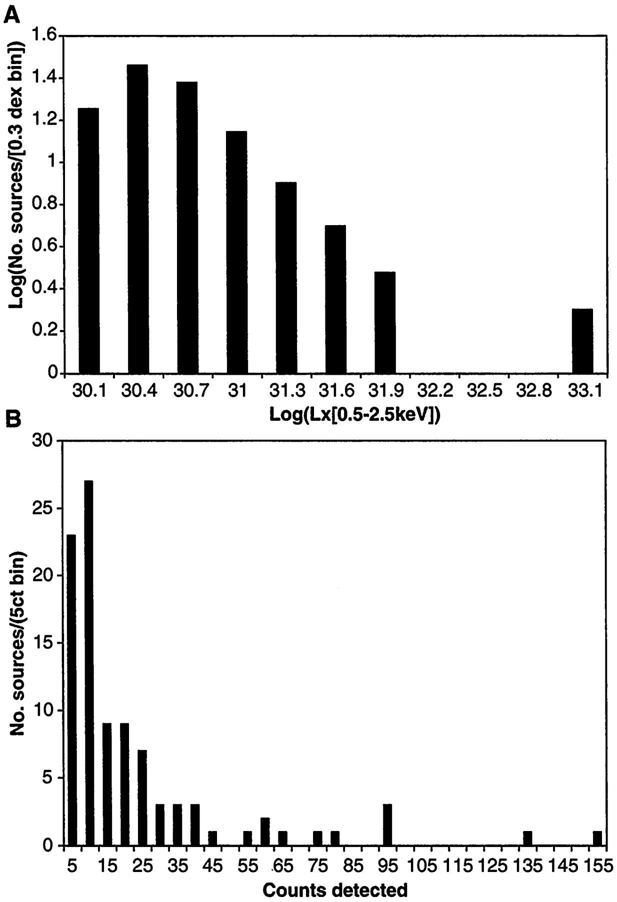

Fig. 2. X-ray luminosity and counts distributions of sources detected with >2.5 cts in central 2′ × 2.5′ of 47Tuc. Counts detected in medium band (0.5 to 4.5 keV) are corrected for instrument and telescope response, 5.0-kpc cluster distance (*16*) and known interstellar absorption of A_V = 0.12 (or equivalent column density NH = 2.4 × 10^{20} cm^{-2}) and an assumed thermal bremsstrahlung spectrum with kT = 1 keV to give source luminosity in the 0.5 to 2.5 keV band for direct comparison with ROSAT results (*14*). The extended energy band of Chandra (0.5 to 8 keV) is utilized for hardness ratio and spectral analysis, which also enable conversion of L_x between the Chandra and ROSAT bands. (**A**) Log source counts versus log L_x, with log L_x value given at the center of 0.3 dex bins. (**B**) Linear source counts versus actual counts detected, with value given at center of 5 ct wide bins. Corresponding log L_x values range from 29.9 to 31.4. The 96 sources plotted in (B) account for only 13% of the total detected x-ray flux from the cluster central region, whereas the brightest two sources (probable quiescent LMXBs X5 and X7) contribute 57% of the total counts.

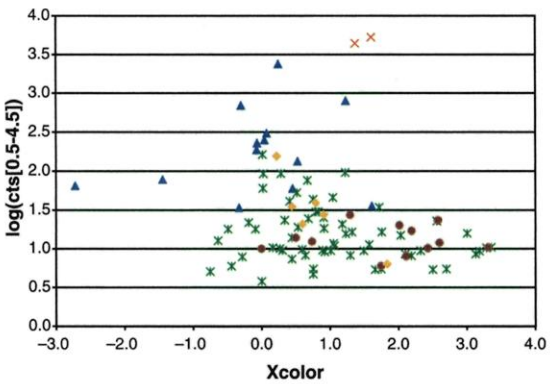

Fig. 3. X-ray brightness (medcts = 0.5 to 4.5keV) versus color [ratio of soft (0.5 to 1.5keV)/hard (1.5 to 6 keV) counts] distribution for sources with medcts ≳ 5 cts. Source types are labeled for the sources identified with 12 MSPs (red ●), 2 quiescent LMXBs (orange ×), 13 CVs (blue △) and 6 M-S binaries (BY Dra systems) in flare outbursts (yellow ◇). The 61 remaining (green *) are unidentified. Source hardness increases to left.

expected [from hard sources in Chandra deep surveys (*26*)] in this 2′ × 2.5′ field and exposure is ≲0.1. However, not only are their power law spectral fits too hard, but our identification (*22*) of both W8 and W15 with blue stars imply x-ray/optical flux ratios similar to values expected for CVs [e.g., $\log(F_x/F_v) = +0.1$ for W15]. X-ray self-absorption is likely in high-inclination CVs (*27*) and may also arise from the "accretion curtain" (*27*), or relatively cool inner disk near the magnetospheric-disk interface suspected to exist in magnetic CVs in which accretion onto the WD is channeled by the magnetic field. Magnetic CVs also typically have relatively high-temperature thermal bremsstrahlung components, though the kT values for X6, in particular, is unusually large.

The brightest CV candidate, X9 (medcts = 2402), is well fit with a thermal bremsstrahlung spectrum with kT = 32 ± 6 keV and is coincident (0.1″) with the blue CV candidate V1 (*28*), confirming the identification by the ROSAT detection (*14*) of X9. The 70 ks Chandra observation of X9 shows evidence for pulsations (false alarm probability $\sim 2 \times 10^{-3}$) with period $P = 218.24$ s and modulation depth 30% (Fig. 4), suggesting this is direct evidence for an accreting magnetic WD and, thus, magnetic CV. Although the total flux from X9 is relatively constant (Fig. 5), and a factor of ~2 fainter than detected with ROSAT, the pulsation amplitude is variable (strongest in the second quarter of the observation) and could instead indicate transient pulsations as found in some CVs (*24*). The faint CV candidate AK09 is also a possible magnetic CV. It was not detected with ROSAT and is too faint even with Chandra (medcts = 36) for spectral fitting but is relatively soft (red) (Fig. 1). The Chandra position is coincident (0.1″) with the blue variable AK09 (*29*) with 1.1-day binary period and was originally suggested (*30*) as the counterpart of the single x-ray source detected in the original Einstein x-ray image of 47Tuc (*5*), for which the positional uncertainty (3″; 90%) would include both X9 and AK09. HST spectra (*31*) now show AK09 to be almost identical to the magnetic CV system GK Per, with similarly long (2 day) binary period and occasional outbursts. AK09 also shows ultraviolet (UV) outbursts (*32*) so that the bright Einstein source, which had both a thermal bremsstrahlung spectrum (kT = 2 to 6 ± 1 keV) as well as possible 120.2-s pulsations (*30*), might have been AK09 in outburst. Both Chandra (*21*) and HST (*22*) studies further constrain the magnetic CV hypothesis.

The optically discovered CV, V2 (*33*), which displays dwarf nova-like outbursts is identified (0.1″) with source X19 and fit with a thermal bremsstrahlung spectrum with kT = 12 ± 6 keV, and the blue variable, V3 (*32*), is the probable counterpart (0.1″) for X10, in contrast to the claim from ROSAT data (*14*). The Chandra spectrum of X10 is unique among all the (moderately) bright sources for which spectral fits were possible. X10 can be fit with a pure power law (α = 2.7 ± 0.2). Its x-ray color and extreme variability, with dips or flares and eclipses (Fig. 5), for which a power spectrum reveals a significant 3.83-hour period, are similar to the quiescent LMXB candidate X5 although a black body plus power law component (as for X5) is only acceptable if a Raymond-Smith component is added in absorption. However, its blue variable counterpart V3, with Balmer emission lines (*34*), suggests accretion is ongoing. We suggest X10, and thus perhaps X5, may be similar to the peculiar magnetic CV AE Aqr, in which spin energy of the WD is partly converted to nonthermal radiation by a magnetic propeller, possibly anchored in the disk (*35*). Alternatively, the power law spectrum suggests X10 might be, as mentioned for X5, an enshrouded MSP.

The fourth group of probable source identifications are main sequence binaries. Of the six sources marked (Fig. 1), the brightest, identified with the 12.7-hour binary E8 (*29*), is the most convincing association with what may be chromospherically active M-S binaries. No blue excess is found in our HST analysis (*22*), and the star appears just above the main sequence. This is as expected for a BY Dra star, the main sequence analog of RS CVn systems in which x-ray emission is produced primarily in giant flare outbursts. Although the $L_x = 10^{31.4}$ erg s^{-1} is a factor of ~10 larger than the maximum found with ROSAT (*36*) for field BY Dra systems in quiescence, this is probably due to what appears to be a smooth decline from a large outburst (Fig. 5). The other five candidate BY Dra systems (Fig. 1) also show x-ray flare-like variations. Using our Chandra-HST astrometry, we have found at least 10 other optical variables without blue excesses that are possible BY Dra systems, although without x-ray flare variations they are less likely identifications. Few, if any, RS CVn systems are seen, with only two to three possible matches (≲0.5″) of Chandra sources with sub-giants.

Implications for population of compact objects, binaries, and cluster core. Although source types for some individual cases are uncertain (e.g., X10), it appears that the 108 sources near the core of 47Tuc are a mixture of four source types. Their quasi-continuous distribution in x-ray colors (Fig. 3) is due to the relative insensitivity of broad-band colors to detailed spectral differences, particularly for multi-component spectra. Nevertheless, some broad differences emerge when the distribution of x-ray color is examined (Fig. 6). Most striking is that most of the MSPs (for which identifications are unambiguous) are relatively soft: 8 of the 12 with medcts ≳5 (and thus rough colors available, as in Fig. 3) are softer than any of the much brighter CV candidates. Similarly, the two most probable quiescent LMXBs are softer than all of the CVs (except AK09) and are intermediate between the CVs and MSPs. The BY Dra candidates (BYs) are intermediate in color but are closer to the CVs. Although the statistics are limited, the values ($\overline{Xcolor}$, σ_{xcolor}) for the mean, $\overline{Xcolor}$, and standard deviation, σ_{xcolor}, for each population are as follows: (1.8 ± 0.3, 0.98), (−0.1 ± 0.3, 1.09), (0.8 ± 0.2, 0.56), and (1.5 ± 0.1, 0.17) for MSPs, CVs, BYs, and quiescent LMXBs, respectively. The corresponding distribution values for the unidentified

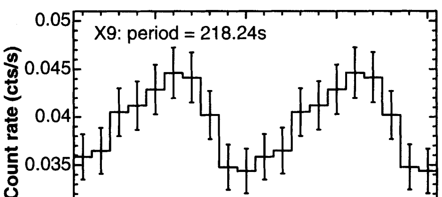

Fig. 4. Folded light curve for the brightest CV candidate, X9, showing its probable detection as a 218.24-s pulsed source and thus identification as an accreting magnetic WD or magnetic CV system (a NS x-ray pulsar with such a long period would be expected only in a wind-fed high-mass x-ray binary found only near regions of massive star formation in the Galaxy, not in globular clusters).

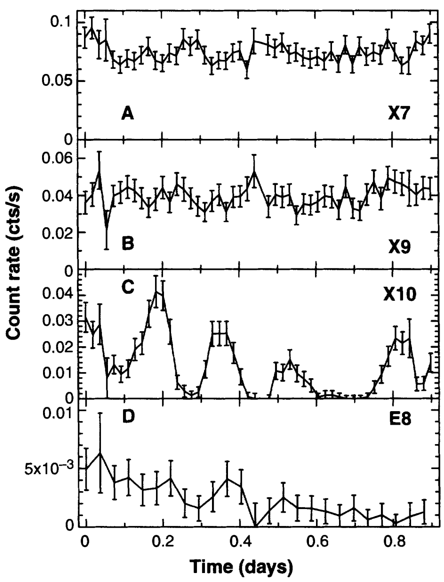

Fig. 5. Light curves, over the full 74-ks (duration) observation, for three of the four source types (all MSP fluxes are constant, within statistics). **(A)** Quiescent LMXB source X7. **(B)** CV candidates X9 (Fig. 4), showing flickering. **(C)** X10, showing dips and eclipses with 3.8-hour period (similar to X5). **(D)** M-S binary candidate E8, showing smooth decline from probable large flare.

(UnID) sources are (1.1 ± 0.1, 1.03), or between the BYs and MSPs. The BY contribution to the UnIDs can be measured by a deep follow-up observation. Most of the same UnID sources will not be detected if they are flare outbursts from BY Dra systems, whereas MSPs will be constant in their x-ray emission. Given the approximate relative numbers of the identified sources and the Xcolor distributions (Fig. 6), we decompose the 61 UnID (>5 ct) source distribution into two quiescent LMXBs, 18 CVs, 11 BYs, and 30 MSPs. Combined with the identified sources, this yields approximate relative (fractional) contributions of 0.04, 0.3, 0.16, and 0.5 for the populations of quiescent LMXBs, CVs, BYs, and MSPs with $L_x \gtrsim 10^{30}$ erg s^{-1}, respectively, where the uncertainties are probably 30%.

We conclude the source population in 47Tuc is dominated by MSPs, with a total number of 45 to 60 in the present Chandra sample (with $L_x \gtrsim 1 \times 10^{30}$ erg s^{-1}). These would naturally account for the background or unresolved red sources, suggesting a still larger MSP population at lower luminosities, if these faint sources are detected as constant flux sources in follow-up observations. Further inferences for the MSP population, including their spin-down energy loss, $\dot{E}$, versus L_x correlations and radial distributions in the cluster, are discussed separately (*19*). However, the CV population may also extend into this faint, soft source background population if there are large numbers of strongly magnetic (AM Her type) CVs for which soft black body emission dominates. These would be optically very faint (like the MSPs), but would display marked variability (relatively long high-low states) and could, thus, also be distinguished from both BY Dra and MSP systems of comparable L_x.

Our estimate that the present sample contains ~30 CVs is ~1/3 the number predicted for tidal capture CV production models (*37*). This may indicate tidal capture is relatively inefficient, but in fact the prediction of a large excess of low luminosity sources ($L_x \lesssim 10^{30}$ erg s^{-1}) may also be consistent with our "background" sources. The size of the CV sample is unexpected because so few dwarf novae have been found (*33*). Combined with the evidence presented here that the brightest CV candidates (e.g., X9) are magnetic CVs, it may be that CVs in globulars are indeed dominated by magnetic systems, as suggested from HST spectra (*38*), in which dwarf nova outbursts are suppressed, at least for short binary period systems.

If only two to three quiescent LMXBs (X5, X7, and possibly X10) are present in the core with the large sample of ~100 MSPs inferred here or from radio counts (*8*), the spin-up time scales for MSPs are reduced to $T_{\rm spinup} \sim N_{\rm quiescent\ LMXBs}/N_{\rm MSPs} \times T_{\rm MSPs}$, where $T_{\rm MSPs} \sim 3 \times 10^9$ years is the typical MSP spin-down age. Thus $T_{\rm spinup} \sim 1 \times 10^8$ years, which is ~10× faster than the $\gtrsim 10^9$ years needed to transfer the $\sim 0.03\ P_4^{-4/3}\ M_\odot$ required (*7*) to spin up the NSs in 47Tuc to their typical ~4-ms spin period (P_4 is the final period in units of 4 ms) at the time-averaged mass accretion rate $\sim 3 \times 10^{-11} M_\odot$ year^{-1}, appropriate to typical LMXBs in clusters with $L_x \sim 10^{36.3}$ erg s^{-1} (*3*) that may be in quiescence ~50% of the time. Thus, the observed quiescent LMXBs are insufficient to support the MSP population, and alternative paths to MSP production may be required such as direct collapse of massive WDs in high CVs (*7*) (for which X9 may be relevant) or MSP formation from common envelope evolution of a NS with a prior generation of ~1 to $3M_\odot$ binary companions, leading to a short-lived NS-WD LMXB phase (*39*).

Lastly, the Chandra image allows the most sensitive mass limits for a black hole in the core of a globular cluster. The precise MSP positions and associated pulsar dispersion measures (*12*) imply an electron density (and thus ionized gas at $T \sim 10^4$ K) of $n \sim 0.1$ cm^{-3} in the cluster core. Bondi-Hoyle spherical accretion with radiative efficiency ε onto a compact object of mass M, radius R, and velocity V in a gas with number density n and sound speed c_s gives an accretion luminosity $L_{\rm acc} = \varepsilon G M^3 m_p n (V^2 + c_s^2)^{-3/2} R^{-1}$, where m_p is the proton mass. For an isolated NS as recently considered for low-luminosity x-ray sources in globulars (*40*), this gives $L_{\rm acc} = 10^{30}$ erg s^{-1}for 47Tuc and appropriate NS values of $M_{\rm ns} = 1.4 M_\odot$, $R_{\rm ns} = 10$ km, $\varepsilon = 0.1$, and $V_{\rm ns} \sim c_s \sim 10$ km/s. If the accretion energy is thermalized over the NS surface, the expected black body spectrum with kT ~ 15 eV is too soft to account for the detected Chandra sources. Although the thermalization process is uncertain, higher temperature radiation from a magnetic pole is also inhibited at such low accretion rates in the spherical case if the NS is rapidly rotating. However, for a black hole, with larger mass $M_{\rm bh}$, emission radius ~3 Schwarzschild radii, and lower equipartition velocity $V_{\rm bh} = V_{\rm ns}(M_{\rm ns}/M_{\rm bh})^{1/2}$ (so that c_s dominates), the accretion luminosity will likely arise from a much lower efficiency flow with $\varepsilon \sim 10^{-4}$ and radiate a much higher temperature spectrum (kT ~ 100 keV), such as calculated in advection (or convection) dominated accretion models (*41*) for accretion on the black hole x-ray source SgrA* in the galactic center. We estimate a soft x-ray luminosity L_x (0.5 to 2.5 keV) ~ $4.5 \times 10^{25}\ \varepsilon_{-4} M_{\rm bh}^2\ T_{100}$ erg s^{-1}, where the uncertain radiation efficiency ε and the spectral temperature T are scaled to 10^{-4} and 100 keV, respectively. The Chandra upper limit of $L_x \sim 1 \times 10^{31}$ erg s^{-1}for the brightest source in the cluster center error circle (*42*) (Fig. 1) implies an upper limit of $M_{\rm bh} \sim 470 M_\odot\ \varepsilon_{-4}^{-1/2}\ T_{100}$. This is consistent with the understanding that binary heating (*2*) prevents core collapse into a moderately massive central black hole and that stellar mass (~3 to 10 $M_\odot$) black holes produced from the initial stars more massive than the NS cutoff have not coalesced in the core but rather have been ejected by the hardest binaries (*43*). A more precise cluster center and accretion model can improve these limits for $M_{\rm bh}$, which are already below the 1700 $M_\odot$ value derived from the central surface brightness profile (*44*). Similar limits for those post core collapse clusters which, like 47Tuc, do not contain a bright LMXB and for which central gas densities could be estimated from MSPs, would be especially interesting.

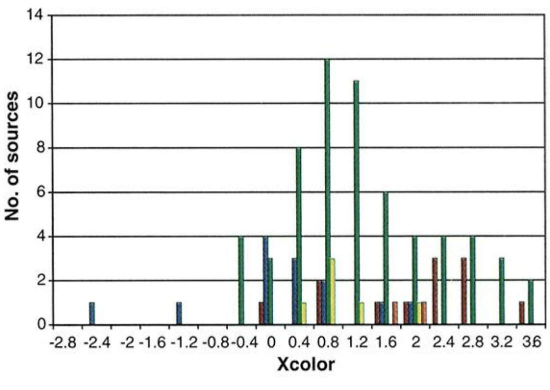

Fig. 6. Distributions of x-ray color (Fig. 3) for 94 sources with medcts ≳ 5 cts and proposed source identifications (see Figs. 1 and 3; source types are color-coded the same as in Fig. 3). M-S binaries are BY Dra systems in flaring outbursts. Means and standard deviations for each source distribution are given in the text.

References and Notes

1. G. Meylan, C. Pryor, *ASP Conf. Series* **50**, 31 (1993).
2. P. Hut *et al.*, *Publ. Astron. Soc. Pac.* **104**, 981 (1992).
3. J. E. Grindlay, *ASP Conf. Ser.* **48**, 156 (1993); L. Sidoli *et al.*, *Astron. Astrophys.*, in press (e-Print available at http://xxx.lanl.gov/abs/astro-ph/0012383).
4. W. Lewin, J. van Paradijs, R. Taam, in *X-ray Binaries*, W. Lewin, J. van Paradijs, E. van den Heuvel, Eds. (Cambridge Univ. Press, Cambridge, 1995), pp. 175–213.
5. Precise (≲3″) x-ray positions for globular cluster LMXBs as measured by J. E. Grindlay, P. Hertz, J. Steiner, S. Murray, and A. Lightman [*Astrophys. J.* **282**, L13 (1984)] enabled mass estimates for the sources and subsequent optical identifications for several as described by L. Homer, S. Anderson, B. Margon, and E. Deutsch [*Astrophys. J.* **550**, L155 (2001) and references therein].
6. G. Clark, *Astrophys. J.* **199**, L143 (1975); J. Katz, *Nature* **253**, 698 (1975).

7. D. Bhattacharya and E. P. van den Heuvel [*Phys. Rep.* **203**, 1 (1991)] provide a comprehensive review of LMXB and MSP evolution. The AIC model for production of MSPs directly from collapse of WDs was proposed to solve the possible LMXB versus MSP birthrate problem in globulars by J. Grindlay and C. Bailyn [*Nature* **336**, 48 (1988)].
8. F. Camilo, D. R. Lorimer, P. Freire, A. G. Lyne, R. N. Manchester, *Astrophys. J.* **535**, 975 (2000).
9. The Chandra X-ray Observatory is described by M. Weisskopf, S. O'Dell, and L. van Speybroeck [*Proc. SPIE* **2805**, 142 (1996)]; the ACIS detector system is described by G. Garmire, J. Nousek, and M. Bautz (in preparation).
10. P. Hertz, J. Grindlay, *Astrophys. J.* **275**, 105 (1983).
11. F. Verbunt, R. Elson, J. van Paradijs, *Mon. Not. R. Astron. Soc.* **210**, 899 (1984).
12. P. C. Freire *et al.*, *Mon. Not. R. Astron. Soc.*, in press (e-Print available at http://xxx.lanl.gov/abs/astro-ph/0103372).
13. The core radius, r_c, is defined as the radius at which the projected surface brightness has decreased by a factor of two from its peak central value. It is a measure of central stellar density and can be related to cluster dynamical parameters [see (*1*)]. The most reliable determination of $r_c = 23''$ for 47Tuc is given by J. H. Howell, P. Guhathakurta, and R. L. Gilliland [*Publ. Astron. Soc. Pac.* **112**, 1200 (2000)].
14. F. Verbunt and G. Hasinger [*Astron. Astrophys.* **336**, 895 (1998)] report the results of the x-ray survey of 47Tuc carried out with the German-U.S. x-ray telescope ROSAT and its HRI detector.
15. Wavdetect is a source detection tool employing wavelet smoothing to match the expected point spread function. Along with the spectral analysis package, Sherpa, used for spectral fits to the brighter ($\gtrsim$300 ct) sources, it is part of the Chandra Interactive Analysis Operation (CIAO) developed by the Chandra X-ray Center (CXC) for analysis of Chandra data and available at http://asc.harvard.edu/ciao/.
16. M. Zoccali *et al.*, *Astrophys. J.* **553**, 733 (2001); e-Print available at http://xxx.lanl.gov/abs/astro-ph/0101485.
17. A two-dimensional K-S test method to detect overlapping but statistics-limited sources has been developed by S. Metchev and J. Grindlay [*Astrophys. J.*, in preparation]; maximum likelihood methods are used in (*14*).
18. W. Becker, J. Trumper, *Astron. Astrophys.* **341**, 803 (1999).
19. J. Grindlay, P. Edmonds. C. Heinke, F. Camilo, P. Freire, in preparation.
20. R. E. Rutledge, L. Bildsten, E. F. Brown, G. G. Pavlov, V. E. Zavlin, *Astrophys. J.*, **551**, 921 (2001); e-Print available at http://xxx.lanl.gov/abs/astro-ph/0012400.
21. C. Heinke, J. Grindlay, P. Edmonds, in preparation. Spectral models fit to the cluster sources included both continuum (black body, bremsstrahlung, and power law) and emission line (Raymond-Smith collisional excitation) models, as provided in the CIAO analysis package [see (*15*)].
22. P. Edmonds, R. Gilliland, J. Grindlay, C. Heinke *et al.*, in preparation.
23. M. Garcia *et al.*, *Astrophys. J.*, **553**, L47 (2001); e-Print available at http://xxx.lanl.gov/abs/astro-ph/0012452.
24. B. Warner, *Cataclysmic Variables*, (Cambridge Univ. Press, Cambridge, 1995).
25. A. Zdjiarski [*ASP Conf. Series* **161**, 16 (1999)] provides a recent review.
26. R. Giacconi *et al.*, *Astrophys. J.* **551**, 624 (2001); e-Print available at http://xxx.lanl.gov/abs/astro-ph/0007240.
27. A. van Teesling, K. Beurmann, and F. Verbunt [*Astron. Astrophys.* **315**, 467 (1996)] suggest absorption by the disk in high inclination nonmagnetic CVs, whereas accretion curtain absorption in magnetic systems is proposed by C. Hellier [*ASP Conf. Ser.* **157**, 1 (1999)].
28. F. Paresce, G. de Marchi, F. Ferraro, *Nature* **360**, 46 (1992).
29. P. Edmonds *et al.*, *Astrophys. J.* **468**, 241 (1996).
30. M. Auriere, L. Koch, S. Ortolani, *Astron. Astrophys.* **214**, 113 (1989).
31. C. Knigge, M. Shara, D. Zurek, K. Long, R. Gilliland, e-Print available at http://xxx.lanl.gov/abs/astro-ph/0012187.
32. D. Minniti *et al.*, *Astrophys. J.* **474**, L27 (1997).
33. M. Shara, L. Bergeron, R. Gilliland, A. Saha, R. Petro, *Astrophys. J.*, **471**, 804 (1996).
34. P. Edmonds *et al.*, in preparation.
35. K. Horne, *ASP Conf. Ser.* **157**, 349 (1999).
36. R. Dempsey, J. Linsky, T. Fleming, J. Schmitt, *Astrophys. J.* **478**, 358 (1997).
37. R. Di Stefano, S. Rappaport, *Astrophys. J.* **423**, 274 (1994).
38. J. Grindlay, *ASP Conf. Ser.* **157**, 377 (1999); P. Edmonds *et al.*, *Astrophys. J.* **516**, 250 (1999).
39. F. A. Rasio, E. D. Phahl, S. Rappaport, *Astrophys. J.* **532**, L47 (2000).
40. E. Pfahl, S. Rappaport, *Astrophys. J.*, **550**, 172 (2001); e-Print available at http://xxx.lanl.gov/abs/astro-ph/0009212.
41. E. Quataert, R. Narayan, *Astrophys. J.* **520**, 298 (1999).
42. D. Calzetti, G. DeMarchi, F. Paresce, M. Shara, *Astrophys. J.* **402**, L1 (1993); G. De Marchi, F. Paresce, M. Stratta, R. Gilliland, R. Bohlin, *Astrophys. J.*, **468**, L51 (1996).
43. S. F. Portegies Zwart, S. McMillan, *Astrophys. J.* **528**, L17 (2000).
44. P. Guhathakurta, B. Yanny, D. Schneider, J. Bahcall, *ASP Conf. Series* **50**, 303 (1993).

45. We thank F. Camilo, H. Cohn, and R. Gilliland for helpful comments. This observation was conducted as part of the GTO program on the Chandra X-ray Observatory with support from NASA (HRC contract NAS8-38248).

28 March 2001; accepted 9 May 2001
Published online 17 May 2001;
10.1126/science.1061135
Include this information when citing this paper.

Spike Transmission and Synchrony Detection in Networks of GABAergic Interneurons

Mario Galarreta[1*] and Shaul Hestrin[1,2]

The temporal pattern and relative timing of action potentials among neocortical neurons may carry important information. However, how cortical circuits detect or generate coherent activity remains unclear. Using paired recordings in rat neocortical slices, we found that the firing of fast-spiking cells can reflect the spiking pattern of single-axon pyramidal inputs. Moreover, this property allowed groups of fast-spiking cells interconnected by electrical and γ-aminobutyric acid (GABA)–releasing (GABAergic) synapses to detect the relative timing of their excitatory inputs. These results indicate that networks of fast-spiking cells may play a role in the detection and promotion of synchronous activity within the neocortex.

In vivo studies indicate that coherent firing among cortical neurons may be related to sensory stimulation and behavioral states (*1*–*4*). However, how postsynaptic cells read out the pattern of activity of their presynaptic axons and how spike synchrony among input axons may be detected by the cortical network remain poorly understood (*3*, *5*).

Studies in intact animals as well as theoretical work suggest that inhibitory interneurons may coordinate neuronal activity in cortical networks (*6*–*11*). Fast-spiking (FS) cells are a prominent subtype of GABA-releasing (GABAergic) interneurons (*12*), exerting powerful inhibitory control of both excitatory and inhibitory cortical cells (*13*–*17*). The properties of excitatory synapses at FS cells (*13*, *18*), as well as their voltage-dependent conductances (*19*–*21*), suggest that these cells may be particularly sensitive to the timing of their inputs, as has been shown for hippocampal interneurons (*22*, *23*). Moreover, cortical networks of FS cells are interconnected by electrical synapses (*14*, *15*, *17*, *24*), and these electrical connections can promote synchronous spiking (*14*, *15*). We investigated how the presynaptic pattern of firing can be transmitted through single-axon pyramidal-to-FS connections and how the degree of synchrony among excitatory inputs may be detected by groups of FS cells.

Precise timing of spike transmission. Pairs of pyramidal and FS cells were recorded in rat neocortical slices (*25*). Monosynaptic pyramidal–FS cell connections were detected by the generation of short-latency unitary excitatory postsynaptic potentials (EPSPs) in response to individual pyramidal spikes (mean latency, 0.63 ± 0.05 ms; range, 0.4 to 1.0 ms; n = 12 pairs) (*26*). To reproduce the ongoing synaptic activity that occurs in vivo (*27*), we injected into the postsynaptic FS cells fluctuating current waveforms that changed from trial to trial, resulting in an irregular firing of ~5 to 50 Hz (Fig. 1A,

[1]Department of Comparative Medicine, [2]Department of Neurology and Neurological Sciences, Stanford University School of Medicine, Stanford, CA 94305, USA.

*To whom correspondence should be addressed. E-mail: galarreta@stanford.edu